

Electrical behaviour of $\text{Bi}_5\text{FeTi}_3\text{O}_{15}$ and its solid solutions with $\text{CaBi}_4\text{Ti}_4\text{O}_{15}$

Carlos Moure*, Luis Lascano, Jesús Tartaj, Pedro Duran

Instituto de Cerámica y Vidrio, CSIC, Camino de Valdelatas, Campus de la Universidad Autónoma de Madrid, 28049 Cantoblanco, (Madrid) Spain

Received 25 January 2002; received in revised form 3 March 2002; accepted 10 May 2002

Abstract

Pure $\text{Bi}_5\text{FeTi}_3\text{O}_{15}$ and $\text{CaBi}_4\text{Ti}_4\text{O}_{15}$ compounds and $(1-x)\text{Bi}_5\text{FeTi}_3\text{O}_{15}-x\text{CaBi}_4\text{Ti}_4\text{O}_{15}$, $x=0.25, 0.50, 0.75$, solid solutions have been prepared by solid state reaction. Ceramics samples with apparent density $>95\%$ D_{th} have been sintered. Their crystalline structure have been determined by X-ray diffraction. Evolution of the lattice parameters has been evaluated. On the pure samples and solid solutions, electrical conductivity and Curie temperature T_c have been measured. Solid solution ceramics were poled and their piezoelectric parameters were established. Pure $\text{Bi}_5\text{FeTi}_3\text{O}_{15}$ showed a high-electrical conductivity behaviour, like that of $\text{Bi}_4\text{Ti}_3\text{O}_{12}$. Electrical conductivity of solid solutions decreases with the $\text{CaBi}_4\text{Ti}_4\text{O}_{15}$ content. Poled ceramic samples showed moderate piezoelectric parameters, and very low values of dielectric loss. A possible conduction mechanism, which differs of that accepted for $\text{Bi}_4\text{Ti}_3\text{O}_{12}$ is discussed.

© 2002 Elsevier Science Ltd and Techna S.r.l. All rights reserved.

Keywords: C. Electrical conductivity; C. Piezoelectric properties; Bismuth titanates

1. Introduction

Bismuth titanates are of great technological interest because of their applications as non-volatile ferroelectric memories [1], and high-temperature piezoelectric materials [2,3]. All of them belong to the Aurivillius bismuth layer-structure, with a general chemical formula $A_{m-1}\text{Bi}_2\text{B}_m\text{O}_{3m+3}$, where A is a large ionic-radius cation, such as K^+ , Ba^{2+} , Sr^{2+} , Ca^{2+} , Pb^{2+} , Bi^{3+} , and B is a small ionic-radius cation, such as Fe^{3+} , Ti^{4+} , Nb^{5+} , W^{6+} , ... The general formula can be developed as follows:

$$A_{m-1}\text{Bi}_2\text{B}_m\text{O}_{3m+3} = (\text{Bi}_2\text{O}_2)^{2+}(\text{A}_{m-1}\text{B}_m\text{O}_{3m+1})^{2-} \quad (1)$$

where $(\text{Bi}_2\text{O}_2)^{2+}$ is a bismuth oxide layer and $(\text{A}_{m-1}\text{B}_m\text{O}_{3m+1})^{2-}$ is a pseudo-perovskite layer; m can vary between 1 and 5 [4]. Most of them show ferroelectric transitions, while some associated families such as $\text{Bi}_2\text{Sr}_2\text{Ca}_x\text{Cu}_{1+x}\text{O}_y$ ($x=0,1,2$), are high-temperature superconducting materials [5].

The compounds with $m=4$, $A=\text{Ba}, \text{Sr}, \text{Ca}, \text{Pb}$, or Bi^{3+} and $B=\text{Ti}^{4+}$, or Fe^{3+} are a subgroup of that compound family. All of them are ferroelectric and have Curie temperatures that ranging from 395°C for $A=\text{Ba}$ to 785°C for $A=\text{Ca}$ [6–8]. Besides that, all show high-resistivity behaviour, except the $\text{Bi}_5\text{FeTi}_3\text{O}_{15}$ compound that shows a higher conductivity [6]. In this compound the Bi^{3+} cation combines with a trivalent cation, Fe^{3+} , to maintain the valence state equilibrium. Those compounds can be described as derived of the three-perovskite-layer $\text{Bi}_4\text{Ti}_3\text{O}_{12}$ compound by the incorporation of a fourth perovskite layer, ATiO_3 , or BiFeO_3 .

The bismuth titanate, $\text{Bi}_4\text{Ti}_3\text{O}_{12}$, compound has good ferroelectric properties, and a relatively high Curie temperature, T_c . Nevertheless, it shows a relatively high, anisotropic, electrical conductivity, which makes very difficult to polarise the ceramic bodies based on this composition [9]. Doping with donors, such as W^{6+} substituting Ti^{4+} leads to a strong increase of the resistivity, allowing a better poling procedure [10]. The $\text{Bi}_5\text{FeTi}_3\text{O}_{15}$ compound shows a very similar behaviour [7]. On the other hand, the $\text{ABi}_4\text{Ti}_4\text{O}_{15}$ compounds, $A=\text{Ba}, \text{Sr}, \text{Ca}$, show very high resistivity values, which allows a good poling process. Thus, the $\text{CaBi}_4\text{Ti}_4\text{O}_{15}$

* Corresponding author. Tel.: +34-91-735-58-52; fax: +34-918-700-550.

E-mail address: cmoure@icv.csic.es (C. Moure).

compound, poled at 250 °C has shown good piezoelectric parameters [11]. This compound sinters at relatively high temperatures, whereas the $\text{Bi}_5\text{FeTi}_3\text{O}_{15}$ compound does at lower temperatures.

The present work is devoted to the study of formation of solid solutions between high-conductive $\text{Bi}_5\text{FeTi}_3\text{O}_{15}$ and low-conductive $\text{CaBi}_4\text{Ti}_4\text{O}_{15}$ compounds, its crystalline and electrical characterisation, piezoelectric properties, and the knowledge of the mechanism that governs the electrical conductivity.

2. Experimental procedures

Pure $\text{Bi}_5\text{FeTi}_3\text{O}_{15}$ (BiFT), and $\text{CaBi}_4\text{Ti}_4\text{O}_{15}$ (CBiT), compounds and solid solutions $(1-x)\text{BiFT}-x\text{CBiT}$, $x=0.25, 0.50, 0.75$, have been prepared by solid state reaction between the corresponding reagent grade oxides and CaCO_3 , with submicronic particle size (Aldrich Chemical Co. Inc., Milwaukee, WI). The weighted powders were homogenised by wet attrition milling, using isopropanol as liquid media. Synthesis was carried out by calcining at 1050 °C, for 2 h. The calcined powders were milled again by impact ball milling and subsequent attrition milling. Compacted pellets were obtained by isostatic pressing at 200 MPa. The sintering was performed at temperatures ranging between 1030 and 1150 °C, for 2 h, except the CBiT compound which was sintered at 1250 °C for 2 h. Density of sintered ceramics was measured by water displacement. Microstructure of the samples was observed on polished and thermally etched surfaces and on fresh fracture surfaces by means of scanning electron microscopy, SEM, (Zeiss DSM 950, Oberkochen, Germany). X-ray diffraction analysis were performed both on the calcined powder and on the sintered samples, using a D-5000 Siemens Diffractometer, (Germany), with radiation K_{α} , and Ni filter. Lattice parameters were evaluated at the following operating conditions: scanning rate 0.25 $2\theta/\text{min}$, and powder of Si as internal standard. The phases were identified using a scanning rate of 2° $2\theta/\text{min}$. The diffraction patterns were indexed as belonging to the space group $A2_1am$ [12]. Sixteen diffraction peaks were used for calculating the lattice parameters by means of a minimum square adjust. Discs were sliced from the sintered samples. Silver electrodes were applied by painting with paste and firing at 700 °C. T_c was evaluated from permittivity-temperature curves taken during heating and cooling. Electrical conductivity against temperature was measured by complex impedance analysis, using an impedance meter, model HP4291A, (Hewlett-Packard, CA, USA). Poling procedure was carried out at 250 °C, in a silicone oil bath, under poling field up to 40 kV/cm; during cooling the applied field was maintained. Piezoelectric constants were evaluated according the IRE Standard, using the same impedance meter, model

HP4291A. d_{33} Values were measured by means of a Berlincourt Piezometer, (model CADT, Channel Inc. OH, USA).

3. Results and discussion

Fig. 1 shows the X-ray diffraction patterns of the different compositions, with $x=0.25, 0.50, 0.75$. As it can be seen, solid solution is fully formed for the three compositions. The very near values of Ca^{2+} (0.126 nm) and Bi^{3+} (0.125 nm) ionic radius favours the formation of solid solution. Table 1 resumes the calculated values of the lattice parameters of solid solutions along with the series ends. The three lattice parameters decrease monotonically with the Ca amount, despite of the slightly higher value of the ionic radius of the Ca cation. The reason can be attributed to the different nature of the external electronic configuration of both cations. Bi^{3+} is a “lone pair” type cation [13]. Its external electronic configuration induces a preferable elongation of the Bi–O bonds in the axial direction, which causes a strong anisotropy in the b direction. On the other hand, Ca^{2+} has a noble-gas external configuration, with high symmetry, and equiaxial Ca–O bonds. The deformation, measured according the a/b ratio diminishes when the Ca content raises. It can be seen as the lattice volume also decreases. Fig. 2 depicts graphically the evolution of the lattice parameters as a function of Ca amount.

Fig. 3 shows several SEM micrographs corresponding to polished surface and fresh fracture surface of the sintered samples. Ceramics sintered at 1050 °C, 2 h showed apparent density ranging between 93% D_{th} for pure CBiT and 97.5% D_{th} for pure BiFT. Thus, it can be said that the incorporation of BiFT to CBiT improves its sinterability. Microstructure of sintered samples is typical of the ceramic materials based on Aurivillius bismuth-layered compounds, with preferential grain

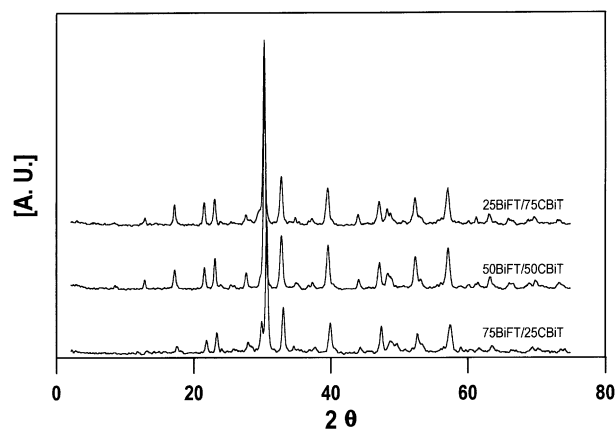


Fig. 1. X-ray diffraction patterns of $(1-x)\text{Bi}_5\text{FeTi}_3\text{O}_{15}-x\text{CaBi}_4\text{Ti}_4\text{O}_{15}$ solid solutions ($x=0.25, 0.50, 0.75$).

Table 1
Lattice parameters of BiFT/CBiT solid solution

Composition	a (nm)	b (nm)	c (nm)	a/b	V (nm ³)
BiFT	0.5479	0.5448	4.129	1.0057	1.232
BiFT/CBiT 75/25	0.5449	0.5434	4.103	1.0028	1.215
BiFT/CBiT 50/50	0.5442	0.5431	4.094	1.0020	1.210
BiFT/CBiT 25/75	0.5431	0.5422	4.081	1.0017	1.202
CBiT	0.5416	0.5408	4.069	1.0014	1.192

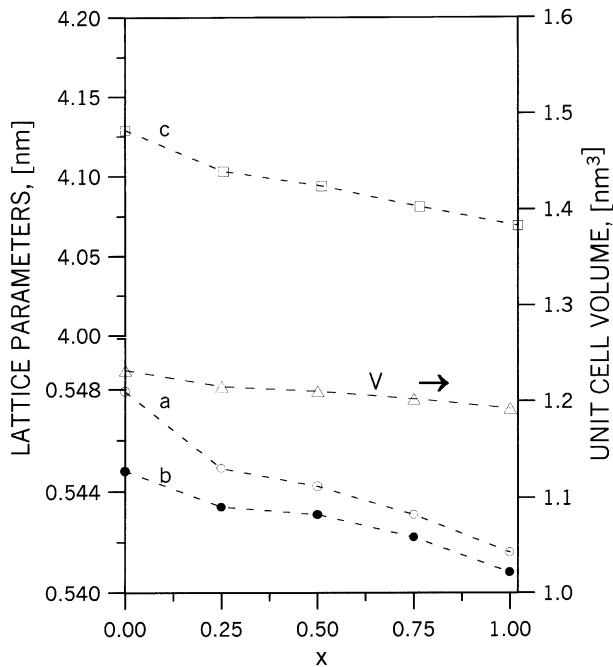


Fig. 2. Evolution of lattice parameters of $(1-x)\text{Bi}_5\text{FeTi}_3\text{O}_{15}-x\text{CaBi}_4\text{Ti}_4\text{O}_{15}$ solid solutions as a function of x .

growth in the ab crystalline plain forming thin platelets, and intergranular porosity with non-rounded shapes. The BiFT sample shows good densification, and a relatively small grain size, with the characteristic platelet-like shape. The incorporation, as solid solution, of CBiT leads to an increase of the grain size and the porosity. The samples show transgranular fracture, such as is seen in the micrographs.

Fig. 4 displays the σT against $1/T$ curves, obtained by complex impedance spectroscopy by sweeping between 0.1 and 10^4 kHz and from room temperature and 800 °C, which is above the Curie temperature of all samples. All the Arrhenius plots are linear, indicating the existence of a small polaron hopping thermally activated mechanism for conductivity. It can be appreciated that the conductivity of BiFT is relatively high, comparable to the corresponding to $\text{Bi}_4\text{Ti}_3\text{O}_{12}$ [14]. The activation energy is also rather similar. The conductivity of the solid solutions decreases and the activation energy increases with the CBiT content, up to reach the very low conductivity value of the pure CBiT compound [11]. Table 2 resumes some data of the electrical behaviour of

the solid solutions. The conductivity has been taken at 300 °C. It can be seen that the conductivity decreases about three orders of magnitude from BiFT to CBiT compounds. Fig. 5 depicts the impedance arcs of the different compositions, taken at 300 °C. The single arc corresponds to bulk conductivity. In this graphic, the strong variation of the electrical conductivity through the system, from BiFT to CBiT can be appreciated.

According to the poling strategy described above, the BiFT sample cannot be poled, because of the very high electrical conductivity at the temperatures necessary to carry out the poling. Attempts to pole at lower temperatures were unsuccessful. All the other compositions were poled successfully. Table 3 resumes some dielectric and piezoelectric parameters measured on the poled samples. As it can be seen, the polarisation is favoured by the presence of CBiT in the solid solution. The piezoelectric parameters are relatively high when compared to those found in other ceramic materials based on Bismuth layer-structure Aurivillius compounds [15,16]. The dielectric losses were very low, <1%, for all the measured samples. The parameters decrease when the CBiT content increases.

Fig. 6a shows the permittivity-temperature curves obtained at a frequency of 100 kHz. As it can be seen in Fig. 6b, the Curie temperature of the solid solutions increases slightly with the CBiT content, having a more strong variation from the 25/75 BiFT/CBiT composition to the pure CBiT compound.

The electrical conductivity of the $\text{Bi}_4\text{Ti}_3\text{O}_{12}$ has been explained by a mechanism of small polaron hopping thermally activated through the Bi^{3+} cations, in a similar manner to the model applied to the electrical conductivity of PZT [17]. According to a detailed structural analysis carried out for Whithers et al., using a bond-valence method, the Bi^{3+} cations in the perovskite layer are overbonded, resulting in a valence state for Bi higher than $3+$ [18]. As consequence, a hopping mechanism between Bi^{3+} and Bi^{4+} through the $(\text{Bi}_2\text{O}_2)^{2+}$ layer or through the perovskite layer could explain the conductivity behaviour [19]. This model also could explain the directionality of the conductivity. The hypothesis of a conduction path through the $(\text{Bi}_2\text{O}_2)^{2+}$ layers has been accepted by some authors [20]. Nevertheless, this hypothesis does not give a satisfactory explanation to the experimental data about the difference of conductivity behaviour of the two pure compound here studied. In fact, the BiFT and CBiT compounds have the same type of structural $(\text{Bi}_2\text{O}_2)^{2+}$ layers, and only small differences in the $(\text{Bi}_2\text{O}_2)^{2+}$ interlayer spacing, due to the difference between the lattice parameters of the respective BiFeO_3 and CaTiO_3 perovskites, can be appreciated. However, a difference between the two compounds exists: Both have three perovskite-like layers, “ BiTiO_3 ”, but the former has a fourth layer, BiFeO_3 , in which a overbonding between

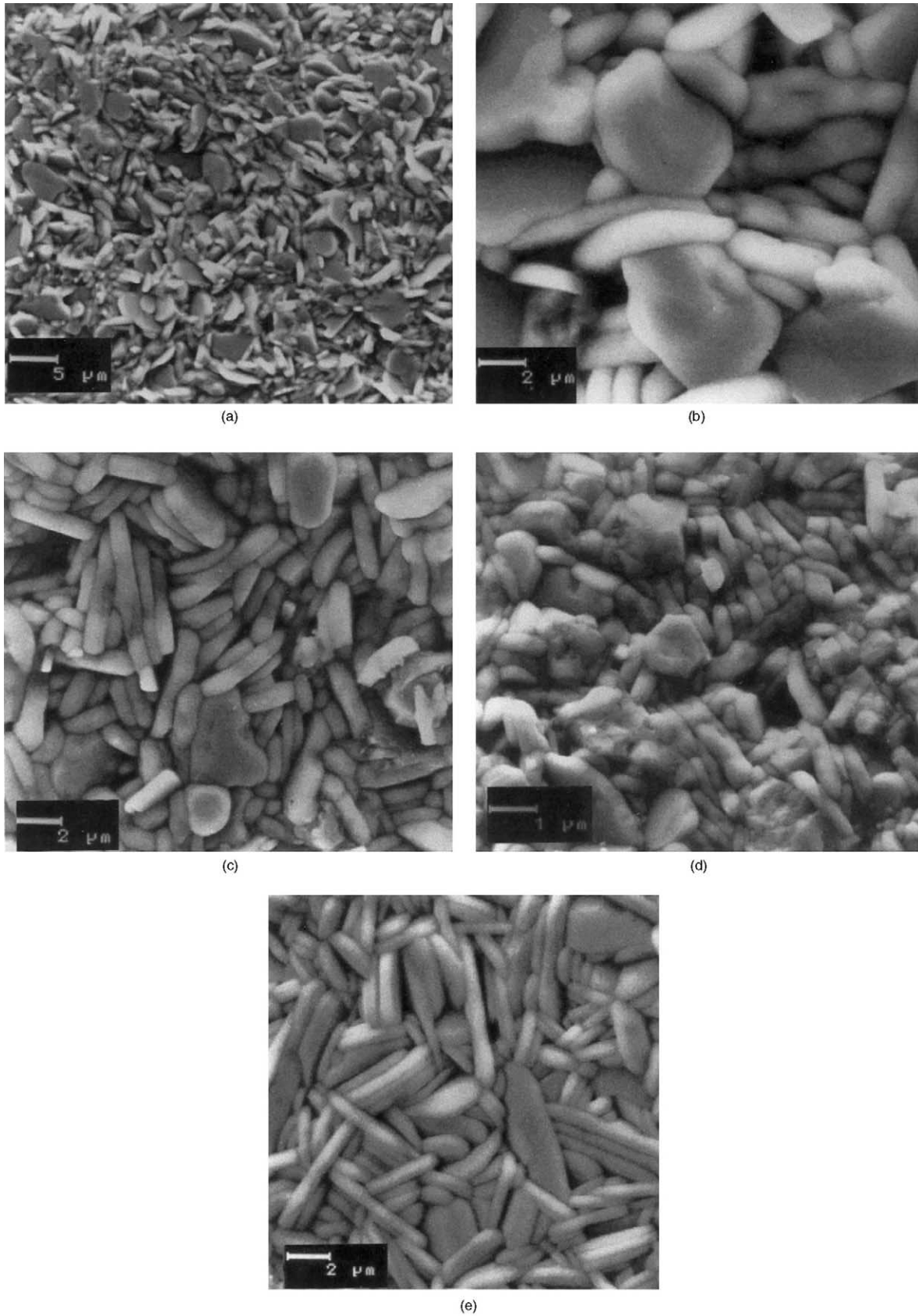


Fig. 3. SEM micrographs of polished surfaces of different ceramic samples, sintered at 1050 °C for 2 h: (a) BiFT, (b) 75 BiFT/25CBiT, (c) 50BiFT/50CBiT, (d) 25 BiFT/75CBiT, (e) CBiT.

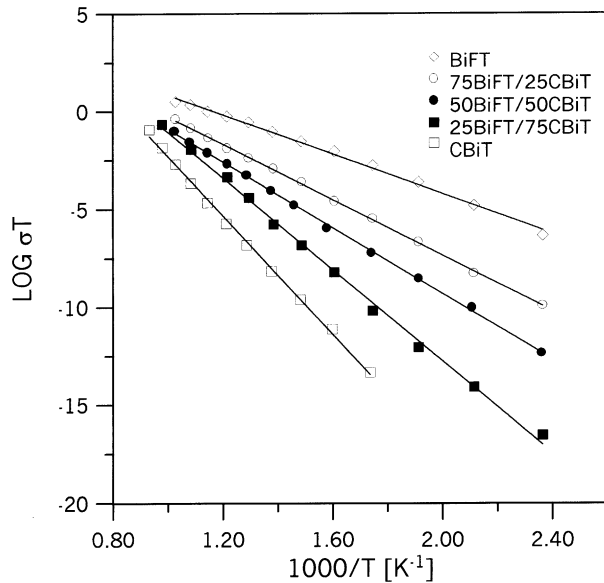


Fig. 4. Variation of σT against $1/T$ of the different compositions, taken from the A.C. impedance curves.

Table 2
Electrical conductivity and activation energy of BiFT/CBiT solid solution

BiFT/CBiT Composition	100/0	75/25	50/50	25/75	0/100
Conductivity $\text{ohm}^{-1}\text{m}^{-1}$, 300 °C	1.39E-3	2.66E-4	5.17E-5	3.01E-5	1.72E-6
Activation energy (eV)	0.56	0.60	0.72	0.77	0.86

Table 3
Dielectric and piezoelectric constants of the BiFT/CBiT solid solution

Compound	K_{33}	$d_{33}(\text{C/N}) \times 10^{12}$	k_t	$\tan \delta$ (%)	f_N
BiFT	—	—	—	—	—
BiFT/CBiT 75/25	96	18.64	0.19	0.96	1831
BiFT/CBiT 50/50	130	11.93	0.14	0.62	2390
BiFT/CBiT 25/75	145	8.68	0.12	0.27	2967
CBiT	110	14.1	0.16	0.31	2460

Bi^{3+} and Bi^{4+} cations, similar to the BiTiO_3 , can occur. On the other hand, in the second compound, a fourth insulating layer, CaTiO_3 is intercalated. Thus, in the BiFT compound, all the perovskite-like layers could show overbonding behaviour, such as it occurs in the $\text{Bi}_4\text{Ti}_3\text{O}_{12}$ compound and, therefore, the electrical behaviour could be very similar, with relatively high-conductivity value. On the other hand, the CBiT has a perovskite layer with very poor conductance. If it is supposed that the electrical conduction path is through the perovskite layers and not through the $(\text{Bi}_2\text{O}_2)^{2+}$ layers, the presence of a perovskite layer of very low conductivity, intercalated between the conductive Bi-containing perovskite layers, could induce a decrease of the total conductivity by trapping of charge carriers. Thus, progressive incorporation of low-conductivity perovskite layers to the compounds containing high-conductive BiTiO_3 layers, substituting to likely conductive BiFeO_3 layers can produce a progressive decrease of the total conductivity of the compounds, such as shown in the present work.

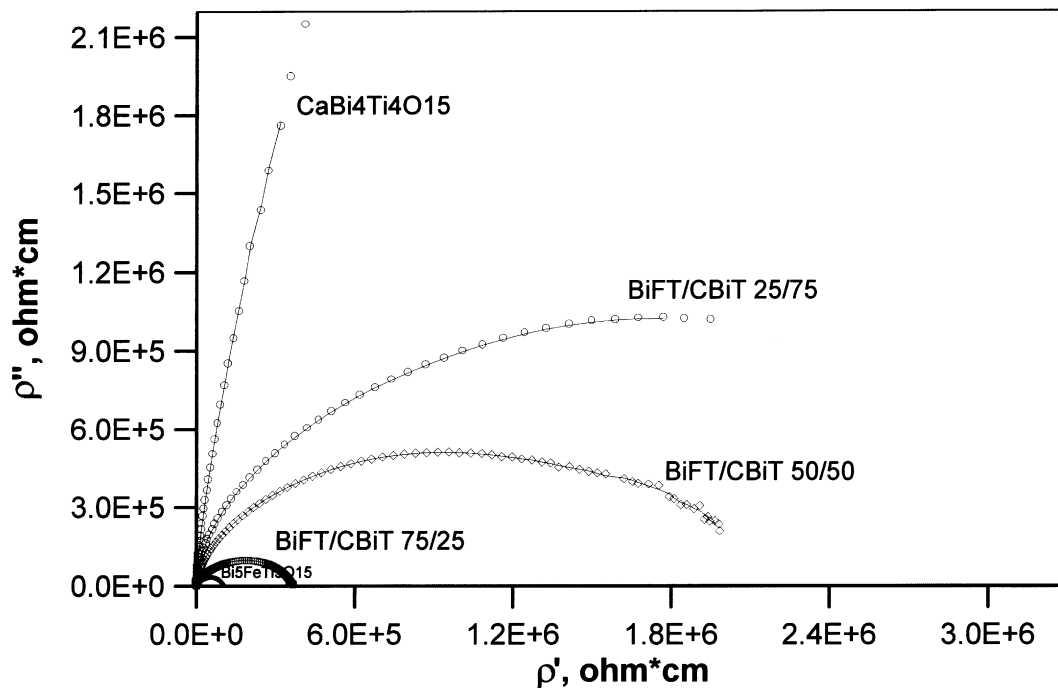


Fig. 5. Impedance arcs corresponding to measurement carried out at 300 °C.

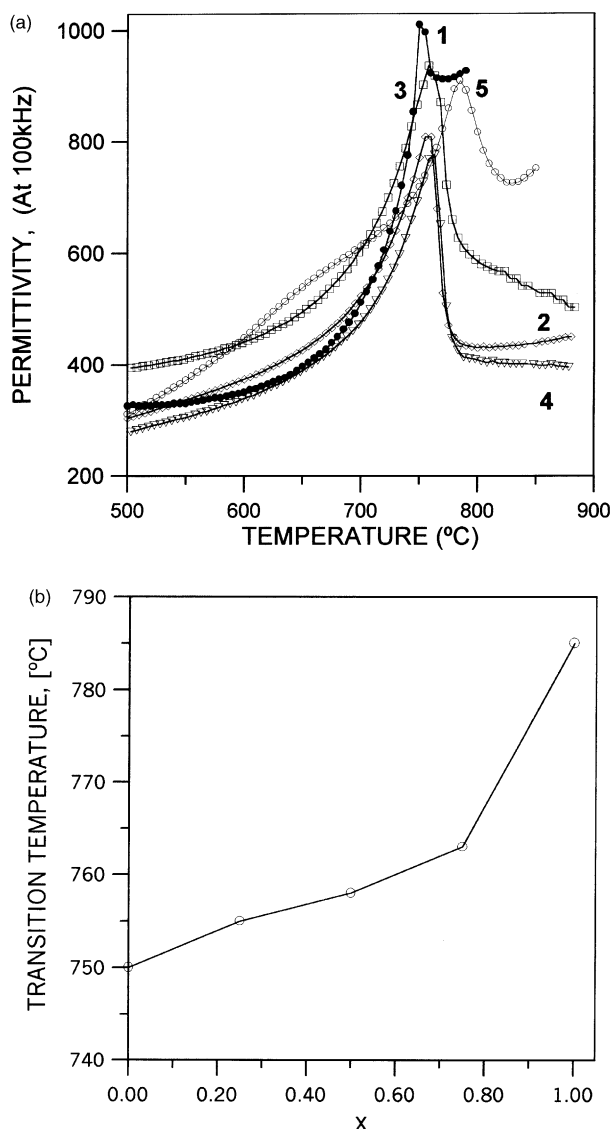


Fig. 6. Results of the permittivity-temperature measurements: (a) Curves permittivity-temperature for the ceramic samples: curve 1, ●-●, BiFT; curve 2, ◇-◇, 75BiFT/25CBiT, curve 3, □-□, 50BiFT/50CBiT, curve 4, ▽-▽, 25BiFT/75CBiT, curve 5, ○-○, CBiT; (b) T_c against temperature obtained from the above curves.

This proposed mechanism could be extended to the electrical behaviour of other bismuth-layered Aurivillius compounds with high conductivity, such as $\text{Bi}_4\text{Ti}_3\text{O}_{12}$, and $\text{Bi}_4\text{Ti}_3\text{O}_{12-n}\text{BiFeO}_3$ series. More work must be done for attaining more sound experimental support to that model.

4. Conclusions

High-conductive $\text{Bi}_5\text{FeTi}_3\text{O}_{15}$ and high-insulating $\text{CaBi}_4\text{Ti}_4\text{O}_{15}$ compounds form a family of solid solutions through the whole range of compositions. The solid solutions sinter at relatively low temperatures with high densification values.

The incorporation, as solid solution of $\text{CaBi}_4\text{Ti}_4\text{O}_{15}$ to the high-conducting $\text{Bi}_5\text{FeTi}_3\text{O}_{15}$ compound decreases strongly its conductivity. According to these results, a novel conduction mechanism is proposed, in which the conduction path is established as being through the perovskite layers, and not through the $(\text{Bi}_2\text{O}_2)^{2+}$ layers. The conduction is argued to be by small polaron hopping through thermally activated Bi^{3+} and Bi^{4+} localised sites, such as has been established previously for other bismuth titanate compounds.

The reduction in the conductivity parameter leads to a higher capacity of the solid solutions to be poled at high temperatures. Piezoelectric parameters decrease with the $\text{CaBi}_4\text{Ti}_4\text{O}_{15}$ content.

References

- [1] S.B. Desu, P.C. Joshi, X. Zhang, S.O. Ryu, Thin films of layered-structure $(1-x)\text{SrBi}_2\text{Ta}_2\text{O}_9-x\text{Bi}_3\text{Ti}(\text{Ta}_{1-y}\text{Nb}_y)\text{O}_9$ solid solutions for ferroelectric random access memory devices, *Appl. Phys. Lett.* 71 (1997) 1041–1043.
- [2] R.C. Turner, P.A. Fuierer, R.E. Newnham, T.R. Shrout, Materials for high temperature acoustic and vibration sensors: a review, *Appl. Acoustics* 41 (1994) 299–324.
- [3] M. Villegas, C. Moure, P. Duran, J.F. Fernandez, Nuevas perspectivas en piezoelectricos de alta temperatura basados en compuestos laminares de bismuto, *Bol. Soc. Esp. Ceram. Vidr.* 36 (1997) 179–184.
- [4] E.C. Subbarao, Systematics of bismuth layer compounds, *Int. Ferroelectrics* 12 (1996) 33–41.
- [5] M. Boekholt, D. Götz, et al., Structural and superconducting properties of $\text{Bi}_{2-x}\text{Pb}_x\text{Sr}_2\text{CaCu}_2\text{O}_{8+\delta}$, *Physica C* 176 (1991) 420–428.
- [6] E.C. Subbarao, Crystal chemistry of mixed bismuth oxides with layer-type structure, *J. Am. Ceram. Soc.* 45 (1962) 166–169.
- [7] I.G. Ismailzade, V.I. Sterenko, F.A. Mirishli, P.G. Rustamov, X-ray and electrical studies of the system $\text{Bi}_4\text{Ti}_3\text{O}_{12}\text{--BiFeO}_3$, *Soviet Phys.-Crystallography* 12 (1967) 400–404.
- [8] L. Lascano, A.C. Caballero, M. Villegas, C. Moure, P. Duran, J.F. Fernandez, Materiales ceramicos texturados $\text{Pb}_x\text{Bi}_4\text{Ti}_{3+x}\text{O}_{12+3x}$ ($x=1,2,3$). Parte II propiedades electricas, *Bol. Soc. Esp. Ceram. Vidr.* 38 (1999) 573–576.
- [9] A. Fouskova, L.E. Cross, Dielectric properties of bismuth titanate, *J. Appl. Phys.* 41 (1970) 2834–2838.
- [10] M. Villegas, A.C. Caballero, C. Moure, P. Duran, J.F. Fernandez, Low temperature sintering and electrical properties of chemically W-doped $\text{Bi}_4\text{Ti}_3\text{O}_{12}$ ceramics, *J. Eur. Ceram. Soc.* 19 (1999) 1183–1186.
- [11] C. Moure, J.F. Fernandez, M. Villegas, P. Duran, Processing and sintering of $\text{CaBi}_4\text{Ti}_4\text{O}_{15}$ powders for high temperature piezoelectric materials, in: E. Gusmano, E. Traversa (Eds.), *Euro-ceramics IV*, vol. 5, Faenza Editrice, Faenza, 1995, pp. 139–144.
- [12] J.F. Dorrian, R.E. Newnham, D.K. Smith, M.I. Kay, Crystal structure of $\text{Bi}_4\text{Ti}_3\text{O}_{12}$, *Ferroelectrics* 3 (1971) 17–27.
- [13] H.S. Brooks, D. Damjanovic, Microstructural control of bismuth titanate based ceramics, in: P. Duran, J.F. Fernandez (Eds.), *Third Euro-ceramics*, Faenza Ed, Iberica, Madrid, 1993, pp. 199–204.
- [14] S.-H. Hong, S. Trolier-McKinstry, G.L. Messing, Dielectric and electromechanical properties of textured niobium-doped bismuth titanate ceramics, *J. Am. Ceram. Soc.* 83 (2000) 113–118.

- [15] F. Chu, D. Damjanovic, O. Steiner, N. Setter, Piezoelectricity and phase transitions of the mixed-layer bismuth titanate niobate $\text{Bi}_7\text{Ti}_4\text{NbO}_{21}$, *J. Am. Ceram. Soc.* 78 (1995) 3142–3144.
- [16] L. Pardo, A. Moure, A. Castro, P. Millan, C. Alemany, B. Jimenez, Microstructure and piezoelectricity of $\text{Bi}_3\text{TiNbO}_9$ ceramics from mechanochemically activated precursors, *Bol. Soc. Esp. Ceram. Vidr.* 38 (1999) 563–567.
- [17] M.V. Raymond, D.M. Smyth, Non-stoichiometry defects and charge transport in PZT, in: O. Auciello, R. Waser (Eds.), *Science and Technology of Electroceramic Thin Films*, Kluwer Academic, Dordrecht, The Netherlands, 1995, p. 315.
- [18] R.L. Withers, J.G. Thompson, A.D. Rae, The crystal chemistry underlying ferroelectricity in $\text{Bi}_4\text{Ti}_3\text{O}_{12}$, $\text{Bi}_3\text{TiNbO}_9$ and Bi_2WO_6 , *J. Solid State Chem.* 94 (1991) 404–417.
- [19] H.S. Shulman, M. Testorf, D. Damjanovic, N. Setter, Microstructure, electrical conductivity and piezoelectric properties of bismuth titanate, *J. Am. Ceram. Soc.* 79 (1996) 3124–3128.
- [20] T. Takenaka, K. Sakata, Grain orientation effects and electrical properties of bismuth layer-structured ferroelectric $\text{Pb}_{(1-x)}(\text{NaCe})_{x/2}\text{Bi}_4\text{Ti}_4\text{O}_{15}$ solid solution, *J. Appl. Phys.* 55 (1984) 1092.